Journal of Nuclear Materials 493 (2017) 40–52

Contents lists available at ScienceDirect

Journal of Nuclear Materials

journal homepage: www.elsevier.com/locate/jnucmat

Radiolysis driven changes to oxide stability during irradiation-corrosion of 316L stainless steel in high temperature water

Stephen S. Raiman [a, *], David M. Bartels [b], Gary S. Was [a]

[a] University of Michigan, 2355 Bonisteel Boulevard, Ann Arbor, MI, 48109, United States
[b] University of Notre Dame, 102 Radiation Research Building, Notre Dame, IN 46556, United States

HIGHLIGHTS

- Stainless steel is irradiated with a proton beam in high temperature water.
- Radiolysis is found to cause an increase in corrosion potential.
- Irradiated oxides were found to be deficient in inner oxide chromium.
- The stability of species in the oxide film is altered due to radiolysis.

ARTICLE INFO

Article history:
Received 3 April 2017
Received in revised form
26 May 2017
Accepted 29 May 2017
Available online 31 May 2017

Keywords:
Stainless steel
Radiation
Irradiation effects
Radiolysis
Passivity
Passive films
Raman spectroscopy
Pourbaix diagram

ABSTRACT

316L stainless steel samples were irradiated with a proton beam while simultaneously exposed to high temperature water with hydrogen (320 °C, 3 wppm H_2, neutral pH) to study the effect of radiation on corrosion. The inner oxides on irradiated samples were found to be depleted in chromium when compared to the inner oxides on unirradiated samples exposed to the same conditions. Additionally, hematite was found on the oxide surfaces of irradiated samples, but not on unirradiated samples. Sample areas which were not directly irradiated but were exposed to the flow of irradiated water also exhibited chromium-deficient inner oxides and had hematite on their surfaces, so it is concluded that water radiolysis is the primary driver of both effects. Thermodynamic calculations and radiolysis modeling were used to show that radiolytic production of hydrogen peroxide was sufficient to raise corrosion potential high enough to cause the dissolution of chromium-rich spinel oxides which make up the inner oxide layer on stainless steel in high temperature water.

1. Introduction

The degradation of stainless steel components in light water reactor cores is of continuing concern to the nuclear power industry. Accurate knowledge of core component lifetimes is required for safe operation and life-extension of the light water reactor (LWR) fleet. Among the life-limiting degradation modes, irradiation assisted stress corrosion cracking (IASCC) is of particular concern for components exposed to radiation. To inform modeling efforts for current reactors, and to aid in the design of new materials, a fundamental understanding of the factors affecting IASCC is needed. Among those factors is the influence of irradiation on the corrosion process.

The effect of radiation on corrosion of LWR core structural components has been a subject of some interest [1–7]. In water, radiation is known to create several strong oxidizing species due to water radiolysis. Further, neutron irradiation may accelerate diffusion of species to the surface and to grain boundaries by creating point defects in the metal and oxide [8]. Prior works have reported on the results of electro-chemical measurements on stainless steel irradiated in LWR environments [9–11]. They did not, however, include a characterization of the oxide film. Other studies have used injected H_2O_2 [12–15] and/or dissolved O_2 [14–17] as a substitute for radiation to increase the corrosion potential of stainless steel in LWR conditions, and have observed changes to the oxide morphology and composition. Kumai and

* Corresponding author.
E-mail address: sraiman@umich.edu (S.S. Raiman).

http://dx.doi.org/10.1016/j.jnucmat.2017.05.042
0022-3115/

Devine [18] found an increased presence of hematite on the oxide surface as dissolved oxygen was added to the corrosive environment. Some works have examined the effect of gamma irradiation on corrosion potential [19,20] and on oxide stability [3], but gamma irradiation does not capture the possible effects of displacement damage. To further the understanding of radiation and corrosion, there is a need to examine the simultaneous effects of radiolysis and displacement damage on the corrosion process.

The objective of this work is to determine how the thermodynamic driving force for corrosion is altered by irradiation. The work focuses on experiments in which stainless steel is irradiated with a proton beam while simultaneously exposed to 320 °C water with 3 wppm H_2. Radiolysis modeling is used to show how irradiation altered conditions at the oxide-solution interface. Oxide films were characterized to determine how the irradiated environment altered the stability of species in the oxide film. Thermodynamic calculations are presented to support a mechanistic explanation of irradiation accelerated corrosion (IAC) in which the spinel oxides on stainless steel in high temperature water dissolve under proton beam irradiation. An accompanying work in this issue examines how irradiation altered the morphology of the oxides on the stainless steel samples, presents kinetic effects of radiation on corrosion, and discusses the possible role of displacement damage as a factor contributing to oxide dissolution during irradiation [21].

2. Experimental method

2.1. Irradiation

Experiments were conducted using the Irradiation Accelerated Corrosion facility at the Michigan Ion Beam Laboratory at the University of Michigan, which was described in detail in a previous work [22]. The facility consists of a 10 mL corrosion cell mounted to the end of a dedicated proton beamline. A schematic drawing of the corrosion cell assembly is shown in Fig. 1. The sample mount was fitted over a hole in the beamline flange and sealed with a Conflat flange on the beamline side, and with a zirconium gasket on the cell side, creating a vacuum seal and a high pressure water seal, respectively. The zirconium gasket was oxidized in an air-filled furnace before use to form a layer of zirconia for electrical isolation. In this configuration, the sample itself was a pressure barrier between the vacuum in the proton beamline, and the high temperature, high pressure water in the corrosion cell.

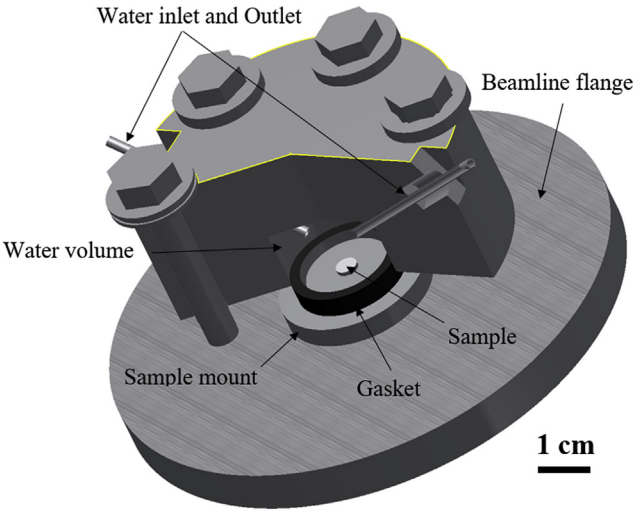

Fig. 1. A schematic drawing of the corrosion cell assembly. The sample mount is compressed between the cell body and the beamline flange, which is attached to the end of the proton beamline. The sample itself is the barrier between the water in the corrosion cell and the beamline vacuum, and functions as a "window" into the corrosion cell through which the proton beam passes. From Ref. [22].

To allow for simultaneous irradiation and corrosion, the proton beam was transmitted through the thin sample, and terminated in the water contained in the corrosion cell. The sample may be regarded as a "window" into the corrosion cell through which the beam transmitted completely (near 100% transmission), so the effects of displacement damage in the sample and radiolysis in the water occurred simultaneously.

The sample was carefully designed to contain the 13 MPa pressure in the corrosion cell while remaining thin enough to allow full transmission of the proton beam. To fabricate the samples, 316L stainless steel sheet (heat 13364044) obtained from Zapp Precision Strip, with a bright annealed finish and a thickness of 49 μm, was cut into discs with a diameter of 7.6 mm. The composition of the 316L stainless steel heat is given in Table 1. To provide the necessary strength to contain the high temperature, high pressure water in the corrosion cell, an area at the center of each disc measuring 3.5 mm was hydraulically formed to a dome shape with a height ~0.8 mm and a thickness of 37 μm, introducing approximately 24% cold work to the material. Samples were then welded around their circumference to a 316L stainless steel sample mount designed to form a high pressure water seal with the corrosion cell, and a high vacuum seal with the beamline. The sample and mount are shown in Fig. 2. To show how proton energy is deposited in the sample and in the water, an ionization plot as calculated by the SRIM code [23] is shown in Fig. 3.

Irradiations were conducted on either a 1.7 MV Tandetron or a 3 MV Pelletron accelerator producing protons at an energy of 3.2 MeV and beam current densities of 1 or 10 μA/cm^2. The raster-scanned beam was transmitted through an aperture with a diameter of either 1 or 2 mm.

The stainless steel corrosion cell contained a ~10 mL volume of pure water with 3 wppm dissolved hydrogen which was constantly refreshed by a flowing water loop at a flow rate of 15 mL/min. Water conductivity and dissolved oxygen (DO) were constantly monitored both upstream and downstream from the cell, and remained at <0.1 μS/cm and <0.5 wppb respectively. Additional details on the corrosion cell and water recirculation system are provided in Ref. [22].

For each irradiation, samples were heated from 25 °C to 320 °C over a period of about 3 h, at which point the proton beam was applied for irradiation periods of 4, 12, 24, or 72 h at a dose rate of 4000 kGy/s measured in the water at the sample surface, and a damage rate to the steel at the sample surface of 7×10^{-6} displacements per atom, per second (dpa/s). The very high dose rate results from the short stopping range of the protons, within about 10 μm of the surface as shown in Fig. 3. One sample was irradiated at a lower dose rate of 400 kGy/s (7×10^{-7} dpa/s) for comparison. Prior testing revealed a sample temperature increase of less than 5 °C at the highest beam current. After irradiation, the beam was turned off and the sample was cooled to 25 °C over a period of about 3 h—25 °C. Control samples were also exposed to the same conditions for 4, 24, and 72 h without irradiation. A list of samples is shown in Table 2.

2.2. Sample characterization

After each experiment, samples were removed from their mounts by grinding away the weld bead. Samples were cleaned by sonicating in a series of acetone, methanol, and ethanol baths for 10 min each.

Samples for transmission electron microscopy (TEM) and